




## Research Article

# Investigation of the material separation behaviour of rocks using scratch tests for the design of tool grinding processes

Berend Denkena<sup>1</sup> · Bernd Breidenstein<sup>1</sup> · Benjamin Bergmann<sup>1</sup> · Philipp Wolters<sup>1</sup> 

Received: 15 January 2022 / Accepted: 11 April 2022

Published online: 28 April 2022

© The Author(s) 2022 [OPEN](#)

## Abstract

The use of natural rocks as cutting tool material poses an environmentally friendly alternative to conventional cutting tool materials. So far, however, the basics of tool grinding processes for rock tools have not been systematically investigated. This study, therefore, presents an investigation of the material removal mechanisms of four different types of rocks and a mono mineral via scratch tests analogous to a face plunge grinding process used in tool grinding. The aim is to contribute to a knowledge-based design of tool grinding processes for rock tools. This also includes a characterization of their mechanical properties. The occurring material removal mechanisms identified by SEM-images as well as width and depth of the scratches are used to evaluate the influence of single grain chip thickness and cutting speed on material removal mechanisms. The results show that ductile material removal is possible for all rocks in certain areas of single grain chip thicknesses ranging from 0.28  $\mu\text{m}$  to 3.75  $\mu\text{m}$  depending on the rock used and the applied cutting speed. Besides this, the results show optima for ductile material removal at single grain chip thicknesses that are up to 87-times higher than predicted by an analytical model. Additionally, recommendations for the design of the tool grinding process of the investigated rocks based on the obtained results are presented.

## Article Highlights

- Investigating material removal mechanisms of rocks against the background of tool grinding.
- Identifying optima of cutting speed and single grain chip thickness for ductile material removal for rocks.
- Contributing to a knowledge-based design of tool grinding processes of rocks.

**Keywords** Natural rocks · Grinding · Scratch tests · Single grain chip thickness

## 1 Introduction

Current challenges such as climate change or economic disruptions create the need to find new ecologically and economically advantageous approaches to meet these challenges. The field of production engineering is no exception. An example of such a new approach from

this field is the use of natural rocks as materials for cutting tools. Although modern cutting tool materials like cemented carbides, polycrystalline diamonds or advanced ceramics provide an advantageous operational behaviour in various applications, they also suffer from ecological and economical disadvantages. The ecological disadvantage of modern cutting tool materials is that their production

✉ Philipp Wolters, wolters@ifw.uni-hannover.de | <sup>1</sup>Institute of Production Engineering and Machine Tools (IFW), Leibniz University Hannover, An der Universität 2, 30823 Garbsen, Germany.



requires large amounts of energy, as is shown for example in [1] for cemented carbides. The associated emission of greenhouse gases contributes to climate change, so a reduction would be beneficial in terms of global climate protection efforts. The economic disadvantage of modern cutting tool materials is that their production, in many cases, requires expensive rare materials with a partially critical availability like cobalt or tungsten. This creates economically and political reasons to recycle or substitute them [2–5]. Natural rocks could therefore provide an ecological and economical advantageous alternative cutting tool material due to their high global availability, low resource prices and low energy tool manufacturing process. Recently, it was shown that it is possible to manufacture indexable inserts from natural rocks and to use them for the turning of aluminium [6, 7]. However, no systematic investigation of the tool grinding process design for manufacturing tools made of rock has yet been carried out.

For a knowledge-based design of grinding processes, it is important to know and understand the occurring material removal mechanisms, as they influence the properties of the workpiece, such as its strength and surface quality. This applies, in particular, to the grinding of hard and brittle materials [8–11]. Responsible for this is the crack initiation and growth associated with brittle material removal in the grinding of hard and brittle materials. These cracks can propagate under load and lead to a failure of the workpiece [12–14]. It is, therefore, necessary to design a grinding process in which ductile material removal mechanisms dominate in order to prevent grinding-induced damage to the rock tools. For this reason, it is necessary to identify the occurring material removal phenomena depending on the grinding parameters. This knowledge enables the design of a suitable tool grinding process for tools made of rocks.

## 1.1 State of the art

In general, two methods are often used to investigate material removal mechanisms in grinding. The first method is the single diamond scratch test. In this method, a tool with a tip consisting of a single diamond is used to indent and scratch the surface of the investigated material under kinematic control [12, 15, 16]. A disadvantage of this method is that it is not possible to investigate the influence of a multiple grain engagement on the material removal. Furthermore, the cutting speed in most scratch tests is up to six magnitudes lower than in conventional grinding processes, though this point can be addressed with a recently developed scratch test [16]. But it is possible to investigate the influence of multiple grain engagements on material removal phenomena by performing quick-stop experiments. This method uses quick-stop devices to perform an interruption of cut in

the grinding process and to “freeze” the chip formation and material removal in the contact zone between tool and workpiece for later investigations. Recently developed quick-stop devices allow interruptions of cut in grinding processes for cutting speeds between 35 and 50 m/s [17]. The disadvantages of this method are the very high necessary experimental and analytical effort to perform these investigations.

However, scratch tests have already been widely used for the investigation of rock cutting processes [18–20], the corresponding material removal mechanisms [20, 21], and the tool-rock interaction [19]. These investigations showed that ductile and brittle material removal mechanisms can occur in the machining of rocks. In literature, it is assumed that it depends on the depth of cut [19], the stress state at the cutting edge [20], and rock stiffness [22] which of these mechanisms dominates in the machining process. The material removal and the occurrence of associated removal mechanisms can be divided into three sub-processes: The first sub-process is the material removal in front and at the sides of the cutting edge, or the diamond tip of a scratch tester in scratch tests. The high negative rake angle at this point causes compressive stress-induced micro and macro shear cracks, which facilitate brittle material removal. Material broken out this way is then pushed from the cutting edge to the sides of the scratch. The second sub-process takes place beneath the cutting edge. The high hydrostatic pressure leads to plastic deformation and compression of the material, which facilitates the formation of plasticised layers and ductile material removal. The third sub-process takes place directly behind the cutting edge. By relieving the pressure induced by the cutting edge, spring-back effects of the material can lead to brittle material removal by chipping if a critical surface pressure is exceeded or ductile material removal if plasticised layers are separated from the material [23]. The grain size of the rocks as well as their cleavage also influences the occurring material removal mechanisms besides the factors mentioned before. Rocks with smaller grain sizes tend to show higher amounts of plastic deformation and, due to this, a higher amount of ductile material removal. The reason for this is that in order to generate the hydrostatic stress field required for the formation of plasticised layers in the rock, contact between the cutting edge and the rock grains must be as direct as possible while at the same time minimising the formation of cracks. The known tendency of coarse-grained rocks to form macro cracks under load leads to the formation of a hydrostatic stress field only selectively and discontinuously, which counteracts plasticisation of the material and ductile material removal. The finer the grain size of the rocks and the lower the amount of macro cracks, the more extensive and continuous is the direct contact between the cutting edge

and the rock grains and thus the hydrostatic stress field, which facilitates ductile material removal. The cleavage of a rock contributes to this relationship as it affects the ease of crack initiation in the microstructure regarding the load direction [23].

But although there are further empirical and analytical studies of rock-tool interaction [24] and material removal mechanisms in rock machining such as through simulation approaches [25] besides scratch test-based investigations, there are currently no studies dealing with these issues against the background of tool grinding of rocks. The reason for this is that most investigations concerned with rocks are linked with issues derived from mining or civil engineering, optimisation of rock cutting processes, or respectively of the tools used for this purpose. The novelty of the investigation of the suitability of rocks as cutting tool material and the manufacture of such tools also contributes to this.

For these reasons, there is currently no systematic investigation of which material properties are important for a suitable design of a tool grinding process for rock tools based on the material removal mechanisms. Findings from a recent investigation, however, indicate a correlation between the grinding result, the critical bending strength, and the properties of the microstructure of the rocks, such as the interlocking of the mineral grains [6]. However, a possible correlation of these rock properties with the material removal mechanisms occurring depending on the selected process parameters was not investigated in this study, nor was an optimised design of the tool grinding process. But it must be mentioned that there are many different methods and approaches to evaluate and describe rock properties in the literature, such as indentation [26], or rebound tests [27], the use of strain–stress curves or mineral composition [28]. Although there are proposals for standardised methods for rock characterisation [29], a wide range of methods and indices is used for this purpose in literature. It is already known in this context that indices and methods developed and used in one field are not generally transferable to other applications or fields [28]. Due to these reasons and the novelty of the application, it is currently unknown which methods can and should be used to characterise rocks for the design of a tool grinding process.

This paper, therefore, aims to contribute to an improved understanding of the tool grinding process of rocks to enable an optimised and knowledge-based design of such processes. For this purpose, scratch tests analogous to a face plunge grinding process are carried out, which is used, for example, for the grinding of indexable inserts. The influence of the cutting speed and the depth of cut on the occurring material removal mechanisms is investigated

to identify possible correlations and use them as potential guidelines for the design of tool grinding processes of rock tools. For this purpose, the paper is structured as follows: The materials and methods used in this investigation are shown in Sect. 2. The results of the investigation are then described in Sect. 3, starting with a characterisation of the rock properties in Sect. 3.1. Subsequently, the results of the scratch tests are shown and discussed in Sect. 3.2. All results are then summarized in Sect. 4.

#### Nomenclature

$a_e$	Depth of cut
$b$	Width of a sample
$b_{dr}$	Active diamond width
$b_r$	Width of a scratch
$E$	Young's modulus
$F_z$	Vertical force
$h$	Height of a sample
$h_b$	Width removal factor
$h_{cu}$	Single grain chip thickness
$h_{cu,hbmin}$	Single grain chip thickness for a minimal $h_b$
$h_{cu,crit}$	Critical single grain chip thickness according to Bifano
$H$	Hardness
$I_{yy}$	Area moment of inertia
$K_{Ic}$	Fracture toughness
$l$	Distance between the bearings of the 3-point bending test
$R_a$	Arithmetic average roughness
$r_d$	Radius of the diamond tip
$v_c$	Cutting speed
$v_f$	Feed velocity
$\alpha$	Inclination angle of the sample
$\sigma_c$	Critical bending strength

## 2 Materials and methods

### 2.1 Rocks

With Alta quartzite, flint, lamellar obsidian, quartz, and Silver quartzite, four different rocks and one mineral are used in this investigation. By this selection, the general rock classes of the metamorphic (Alta quartzite, Silver quartzite), the sedimentary (flint), and the igneous rocks (lamellar obsidian) are included in this investigation. These rocks have also already been used and characterised in a previous investigation of the suitability of rocks as cutting tool materials [6]. A DEMA WB 2000 rock saw and a Struers Discotom-10 cut-off grinding machine are used to cut 40

samples of each rock with dimensions of  $32 \times 22 \times 22$  mm from the raw rocks. The used rocks had various shapes and dimensions before cutting, ranging from blocks and nodules with lengths of 80–250 mm to slabs up to 22 mm thick. Subsequently, the samples are ground to the dimensions  $30 \times 20 \times 20$  mm on a Rödgers RFM 600 DS machine tool using a grinding tool with metallic bond and diamond as abrasive with a grain size of D46 (38 to 45  $\mu\text{m}$ ) and a grain concentration of  $3.3 \text{ g/cm}^3$  (C75). The grinding process is performed with a cutting speed of 30 m/s, a feed velocity of 24 mm/min, and a depth of cut of 0.1 mm. All samples are then polished on a Buehler EcoMet 30 in five steps with silicon carbide with the grain sizes P120 (125  $\mu\text{m}$ ), P240 (58.5  $\mu\text{m}$ ), P400 (35  $\mu\text{m}$ ), P800 (21.8  $\mu\text{m}$ ) and P1200 (12.6  $\mu\text{m}$ ) to achieve a low surface roughness of the samples. Tactile surface roughness measurements of five samples for each rock with a Mahr Perthometer PGK showed an arithmetic average roughness Ra between 0.045  $\mu\text{m}$  (obsidian) and 0.372  $\mu\text{m}$  (Silver quartzite) after polishing.

Besides this, samples of all rocks are cut for the conduction of hardness measurements and 3-point bending tests to evaluate the critical bending strength. These samples are cut to dimensions of  $18 \times 18 \times 5.5$  mm using the machines mentioned previously. During cutting, care is taken to ensure that existing mica textures in the quartzite samples are aligned perpendicular to the load direction of the 3-point bending tests. Subsequently, the samples were ground to a thickness of 4.76 mm using a 5-axis Blohm Profimat MC 407 grinding machine and a grinding tool with a metallic bond, diamond as abrasive, a grain size of D46, and a grain concentration of  $4.4 \text{ g/cm}^3$  (C100). The grinding process is performed in two steps: In the first step, rough machining is carried out with a cutting speed of 30 m/s, a feed velocity of 3200 mm/min, and a depth of cut of 20  $\mu\text{m}$  until the samples have reached a thickness of 4.78 mm. After this, a finishing operation is performed using the same cutting speed, a feed velocity of 200 mm/min, and a depth of cut of 5  $\mu\text{m}$ . Three samples of each rock are manufactured for the hardness measurements and 30 for the conduction of the 3-point bending tests. The tactile measured arithmetic average roughness of the samples after grinding with the corresponding standard deviations is shown in Table 1.

## 2.2 Characterisation of rock properties

A Struers Duramin hardness tester is used to investigate the hardness of the rocks via Vickers hardness tests (HV1). To identify possible thermal influences on hardness, the samples are tested at 25, 50, 100, 150, 200 and 250  $^{\circ}\text{C}$ . The heating of the samples is done with a

**Table 1** Roughness of the samples for hardness measurements and 3-point bending tests after grinding

Rock	Arithmetic average roughness Ra in $\mu\text{m}$
Alta quartzite	$0.89 \pm 0.07$
Flint	$0.48 \pm 0.04$
Lamellar obsidian	$0.49 \pm 0.12$
Quartz	$0.60 \pm 0.13$
Silver quartzite	$1.17 \pm 0.20$

Phoenix Instrument RSM-10HP heating plate. A Testo PT100 surface probe is used to measure the temperature of the samples. For each rock, a total of fifteen measurements is conducted for each temperature. Five measurements are taken on each of the three samples of each rock. Each sample is heated again after every indentation to ensure hardness testing at the desired temperature. Besides this, after testing the samples at 25  $^{\circ}\text{C}$ , the Vickers indentation samples are used to determine the fracture toughness  $K_{Ic}$  via the Palmqvist method. Furthermore, an Agilent Technology G200 Nanoindenter with a Berkovich tip is used to determine Young's modulus of the rocks at 25  $^{\circ}\text{C}$  via nanoindentation. For this purpose, 49 indentations with an indentation depth of 2000 nm are performed for each rock.

The determination of the critical bending strength via 3-point-bending tests is based on DIN EN 843-1 [30]. The critical bending strength can be used as a measure of the load-bearing capacity and structural cohesion of solids with several phases. It has already been used for describing the load-bearing capacity of rocks [6] and grinding wheel bonds [31]. Assuming that the area moment of inertia  $I_{yy}$  of the samples can be calculated with Eq. (1) using the width  $b$  of 18 mm and the height  $h$  of 4.76 mm, the critical bending strength  $\sigma_c$  can be calculated according to Eq. (2).

$$I_{yy} = \frac{b \times h^3}{12} \quad (1)$$

The distance  $l$  between the bearings of the 3-point bending test is constantly 13 mm. The acting vertical force  $F_z$  is measured with a Kistler 9257B dynamometer.

$$\sigma_c = \frac{3 \times F_z \times l}{2 \times b \times h^2} \quad (2)$$

To identify potential thermal influences on the critical bending strength, the bending tests are conducted at the same temperature levels as the hardness tests. Five samples are tested for each temperature level.



The heating of the samples is done in the same way and with the same equipment used in the hardness measurements.

### 2.3 Experimental setup of the scratch tests

All experiments are conducted on a 5-axis Blohm Profimat MC 407 grinding machine. The machine has an axis resolution of  $0.1\ \mu\text{m}$  and an input resolution of one micrometer for the linear axes. Besides that, it has a positioning accuracy of  $0.001^\circ$  for the rotational axes. The experimental setup of the scratch tests is shown in Fig. 1. The kinematics of the setup is analogous to that of a plunge face grinding operation which is a commonly used grinding operation for the manufacture of indexable inserts. Therefore, the depth of cut of a scratch is constant over the width of the sample and is simultaneously equivalent to the single grain chip thickness  $h_{\text{cu}}$  of the process. Scratch testers with a diamond tip with a Rockwell geometry and a tip radius  $r_d$  of  $200\ \mu\text{m}$  are used as scratching tools. The clearly defined tip geometry offers the advantage of increased reproducibility and traceability of the results. The scratch testers are mounted in an aluminium carrier disc with a diameter of  $400\ \text{mm}$  and a height of  $20\ \text{mm}$ . The way the scratch testers are mounted ensures that the (111)-plane of the diamond tip is aligned parallel to the cutting speed  $v_c$  to ensure a high load-bearing capacity and low wear of the diamond tip. The carrier disc with mounted scratch tester is balanced to a quality of G 1.6 according to ISO 21940-11 [32].

To investigate the influence of cutting speed and single grain chip thickness on the material separation behaviour of the rocks, these parameters are varied in three and four levels, respectively. The process parameters are shown in Table 2. The feed velocity of the process is selected depending on cutting speed so that the distance between

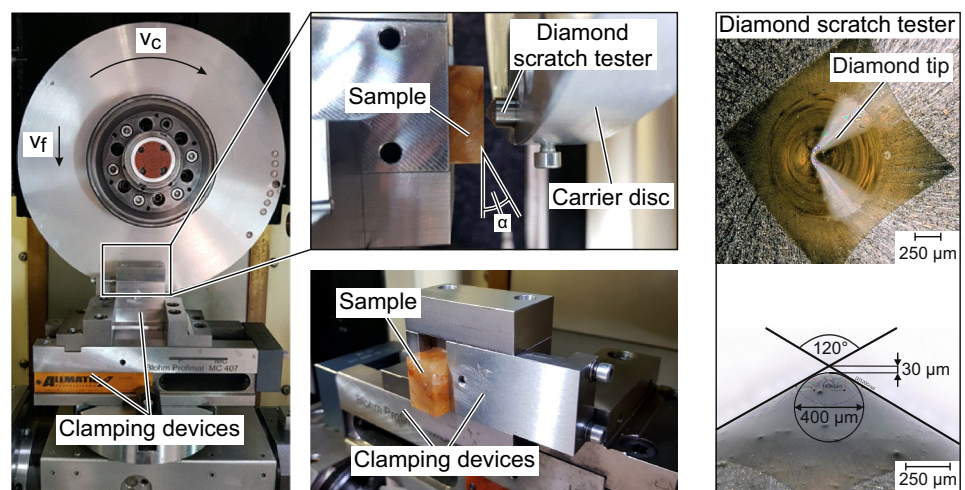
**Table 2** Process parameters of the scratch tests

Process variables	Levels
Cutting speed $v_c$ in m/s	15; 30; 40
Depth of cut $a_e$ in $\mu\text{m}$	1; 2; 3; 4
Feed velocity $v_f$ in mm/min	760; 1550; 2050
Inclination angle $\alpha$ in $^\circ$	0; 0.023

individual scratches is one millimetre in order to avoid mutual interferences of the scratches. Because of that, the feed velocity is not varied independently from the other parameters. Furthermore, the experiments are conducted with or without an inclined sample for all parameter variations. The experiments are repeated once for the samples without an inclination. The inclination angle  $\alpha$  is always  $0.023^\circ$  for the inclined samples. The benefit of inclining the samples is that the depth of cut increases in feed direction by  $0.4\ \mu\text{m}$  for each scratch due to the inclination and the distance between the scratches. This, in combination with the experiments without an inclination angle, enables a more finely resolved analysis of the influence of the depth of cut on material separation. Five parameter combinations with one experiment each are performed with one scratch tester to limit the number of scratch testers needed for this investigation. The wear of the scratch testers is checked after each experiment. If the tip radius is found to be worn more than  $1\ \mu\text{m}$ , the scratch tester is no longer used, and the corresponding test is repeated with a new scratch tester. In addition, scratches that show a significant deviation from the intended depth of cut are excluded from the evaluation of the experiments. A total of 240 scratches per rock is included in the evaluation of the experiments.

After the scratch tests, a Keyence VHX 500 digital microscope is used to evaluate the width of the scratches. The

**Fig. 1** Experimental setup of the scratch test



Wol/103587 © IFW

depth of the scratches and thus the actual depth of cut of the scratch tester for each scratch was measured with a Confovis DuoVario confocal microscope. The software MountainsMap® was used to analyse the measurement data of the confocal microscope. Besides that, a Zeiss EVO 60 XVP (tungsten cathode) scanning electron microscope was used to make SEM-images of the scratches for a closer investigation of the occurring material removal phenomena. To provide an overview of the procedure and scope of the investigations carried out, Fig. 2 summarizes the sequence of investigations in the form of a flow chart.

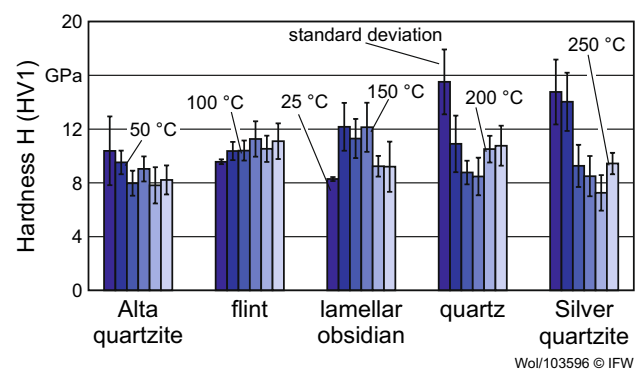


Fig. 3 Vickers hardness of the rocks at different temperatures

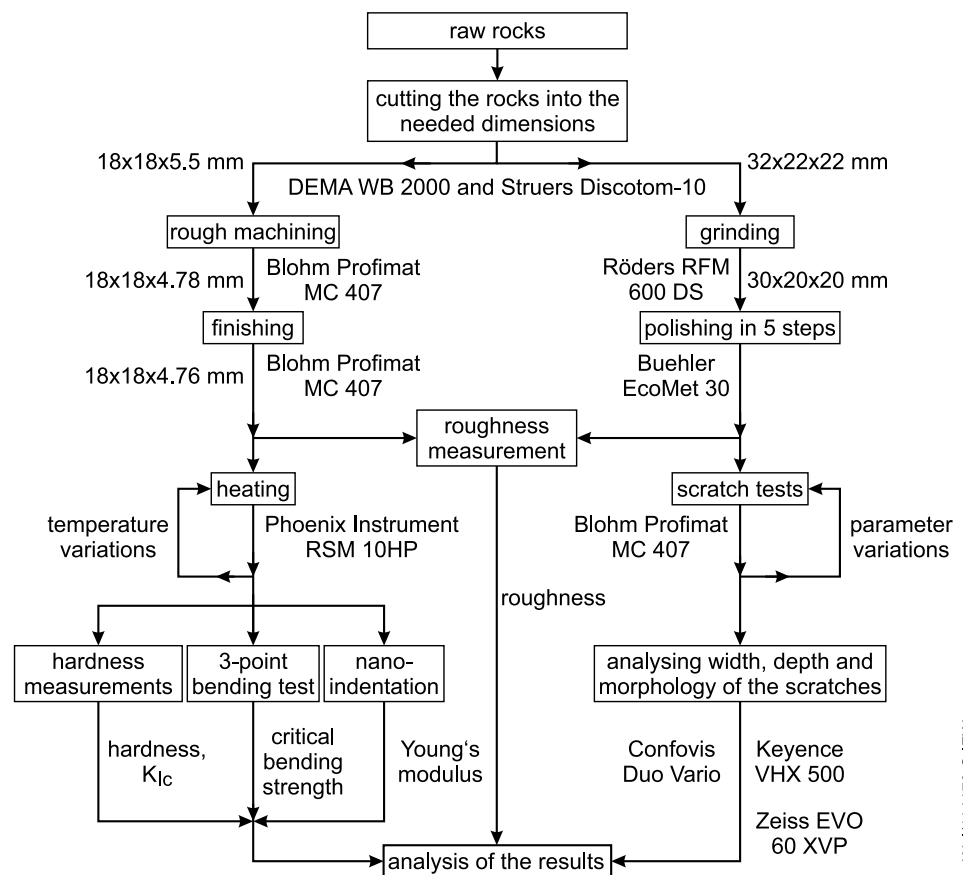
### 3 Results and discussion

#### 3.1 Properties of the rocks

The hardness and critical bending strength of the rocks at different temperature levels are shown in Figs. 3 and 4. The hardness of the rocks at 25 °C is between 8.29 GPa (lamellar obsidian) and 14.76 GPa (Silver quartzite). The results show an influence of the temperature level on rock hardness, as shown in in Fig. 3. However, the influence of temperature on hardness differs for the rocks. While Alta quartzite, quartz, and Silver quartzite show

a tendency to decrease in hardness at higher temperatures, the opposite is true for flint and obsidian. These two rocks show an increase in hardness at higher temperatures, with obsidian having a hardness peak at temperatures between 50 and 150 °C. The hardness of these two rocks, therefore, increases between 17.7% (flint) and 46.9% (lamellar obsidian), while for the other rocks hardness reduces up to 55.8% (quartz). Concerning critical bending strength, the general influence of the temperature level is comparable for all rocks. Starting at values

Fig. 2 Flow chart of the procedure of the experiments



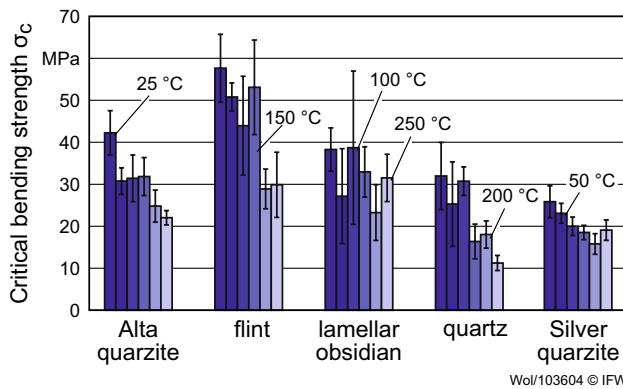


**Fig. 4** Critical bending strength of the rocks at different temperatures

between 25 and 58 MPa (Silver quartzite and flint), all rocks show a decrease in critical bending strength between 38.9% (Silver quartzite) and 64.9% (quartz) at maximum. With temperature increase, structural cohesion and load bearing capacity decrease in all rocks studied. Hardness, however, is increased or decreased depending on the rock. Considering that these factors are relevant to the material removal mechanisms, a variation in thermal loads (e.g., due to a variation of  $v_c$ ) in the scratch tests may affect results based on these effects.

Possible explanations for the observed trends with a temperature increase are a softening of the rocks, a change in the existing stress states and different thermal expansions of the individual mineral phases. A change in existing stress states from compressive to tensile, for example, can facilitate crack propagation while different thermal expansions of various mineral phases in the rocks can lead to crack initiation. Both factors weaken the structural cohesion tested in the 3-point bending tests and therefore reduce the resulting critical bending strength. The partially high standard deviation at all temperature levels for hardness and critical bending strength is a result of the natural variability of the amounts of the mineral phases which form the rocks. The different mineral phases in the rocks can not only have different hardness values (e.g., quartz and mica layers like muscovite in the quartzites), but they can also have different load-bearing capacities which can influence the load-bearing capacity of the microstructure as a whole. The same applies to existing stress states in the rocks which are influenced by their formation process.

Furthermore, fracture toughness  $K_{Ic}$  and Young's modulus of the rocks at 25 °C with their respective standard deviations are given in Table 3. The measured fracture toughness of the rocks between 1.91 and 2.89  $\text{MPa}\cdot\text{m}^{1/2}$  is comparable to the respective values of technical

**Table 3** Fracture toughness and Young's modulus of the rocks at 25 °C

Rock	Fracture toughness $K_{Ic}$ in $\text{MPa}\cdot\text{m}^{1/2}$	Young's modulus $E$ in GPa
Alta quartzite	$1.91 \pm 0.23$	$94.7 \pm 11.3$
flint	$2.89 \pm 0.43$	$88.8 \pm 2.4$
lamellar obsidian	$2.17 \pm 0.19$	$74.4 \pm 0.8$
quartz	$2.31 \pm 0.24$	$102.7 \pm 3.3$
Silver quartzite	$2.37 \pm 0.38$	$102.4 \pm 4.9$

ceramics, such as alumina- or magnesia-based ceramics [34]. But compared to these technical ceramics, Young's modulus of the rocks is up to six times lower. It is instead comparable to ceramics like mullite or steatite [35].

### 3.2 Results of the scratch tests

In addition to SEM-images, the width removal factor  $h_b$  defined by *Apmann* [33] is used to analyse and allocate material removal that occurs as a function of the selected process parameters in the scratch tests. The width removal factor is the ratio between the width of a scratch  $b_r$  and the active width of the diamond tip of the scratch tester  $b_{dr}$ , as shown in Fig. 5 and Eq. (3).

$$h_b = \frac{b_r}{b_{dr}} \quad (3)$$

The active width of the diamond tip  $b_{dr}$  can be calculated for an  $a_e$  up to 25  $\mu\text{m}$  with Eq. (4) by using the radius  $r_d$  of the diamond tip of the scratch tester:

$$b_{dr} = 2 \times \sqrt{r_d^2 - (r_d - a_e)^2} \quad (4)$$

The more pronounced the material removal during the scratch tests is determined by brittle material removal, the greater the width removal factor becomes, as the width of the scratch increases due to brittle breakouts at the edges of the scratch while the active width of the diamond tip remains constant. The more ductile the material removal, the more the width removal factor converges to the value one, as  $b_r$  and  $b_{dr}$  converge (see Fig. 5). Therefore, it can be assumed that  $h_b$  can be used as an indicator for the occurring material removal mechanism. However, it must be taken into account that ductile material removal phenomena such as ploughing can create material accumulations on the sides of the scratch by displacing material, which in turn can lead to a perceived higher width of the scratch during evaluation. This can lead to the calculation of a higher width removal factor without the occurrence of

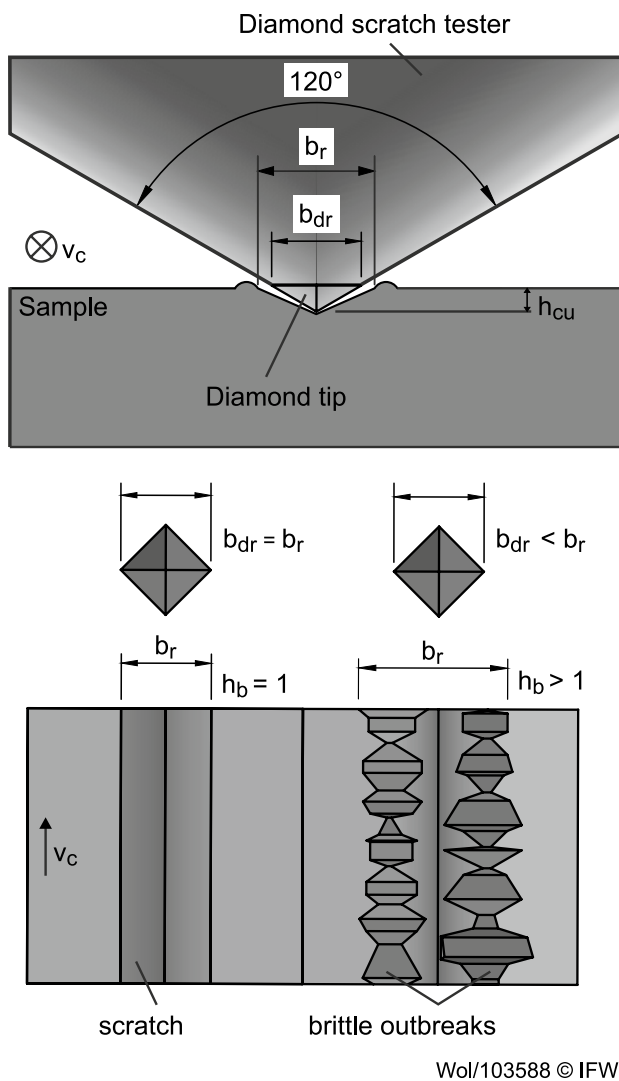


Fig. 5 Width removal factor  $h_b$

brittle material removal and must therefore be taken into account as a potential error source when using this factor as a criterion for evaluation of the results.

In Fig. 6, width removal factors of the rocks resulting from the scratch tests are shown for a cutting speed of 30 m/s along with their respective standard deviations. Due to a large number of investigated scratches, the mean value of the results from intervals of the single grain chip thickness with a width of 0.5  $\mu\text{m}$  each is shown with the associated standard deviation for greater clarity. For flint, no scratches with a depth of cut for the intervals from 2.5–3.0  $\mu\text{m}$  and 3.0–3.5  $\mu\text{m}$  could be found in the analysis. The scratches produced in the respective experiments showed a slightly lower depth of cut than 2.5  $\mu\text{m}$  in the first case and a slightly higher depth of cut than 3.5  $\mu\text{m}$  in the second case. Considering the scale of the depth of cut used in this study, minimal deviations ( $< 1 \mu\text{m}$ ) in the

surface height or flatness of the samples used could be a possible explanation for the deviation in the depth of cut measured after the experiments.

The results of the scratch tests show a correlation between the single grain chip thickness and the width removal factor. For Alta quartzite, quartz, and Silver quartzite, a decrease in the width removal factor and, therefore, a more pronounced ductile material removal for an increase of single grain chip thickness can be observed until the width removal factor reaches a minimum. After that, a further increase of single grain chip thickness leads to an increase in the width removal factor. For the quartzites, this minimum is at a single grain chip thickness between 1.0 and 1.5  $\mu\text{m}$ , while for quartz, this minimum is at a single grain chip thickness between 1.5 and 2.0  $\mu\text{m}$  for the given cutting speed. A decrease of the width removal factor for increasing single grain chip thicknesses can also be detected for flint. Contrasting to the rocks mentioned before, no minimum of  $h_b$  with a subsequent increase of this factor could be observed for flint in the investigated interval of the single grain chip thickness. Furthermore, neither microscope nor SEM-images show signs for intensive brittle outbreaks for lower single grain chip thicknesses. Therefore, it is possible that material removal, in this case, is dominated by ductile mechanisms which, at lower single grain chip thicknesses, displace the material to the sides of the scratch. This widens the scratch and thus increases  $h_b$ , while higher single grain chip thicknesses lead to chip formation in front of the indenter. The high critical bending strength of flint compared to the other rocks supports this hypothesis due to the associated increased load-bearing capacity of the microstructure, which favours ductile material removal and chip formation. For lamellar obsidian,  $h_b$  remains nearly constant for higher single grain chip thicknesses and only shows a decrease for single grain chip thicknesses higher than 2.5  $\mu\text{m}$ .

Based on these observations, it can be assumed that there is a rock-specific critical single grain chip thickness beyond which a change in material removal mechanisms from brittle to ductile occurs as it is known for other materials. However, the results also indicate that a single grain chip thickness below a critical value does not necessarily lead to ductile material removal. The results allow the hypothesis that the material removal is mainly ductile in a certain range around a critical single grain chip thickness and mainly brittle outside this range, regardless of whether it is exceeded or not. The basics of material removal for rocks described before are a possible explanation for this. As described before, ductile removal in rock machining correlates with the stress state at the cutting edge and the occurrence of a suitable hydrostatic stress state in the material. It can be assumed that a variation



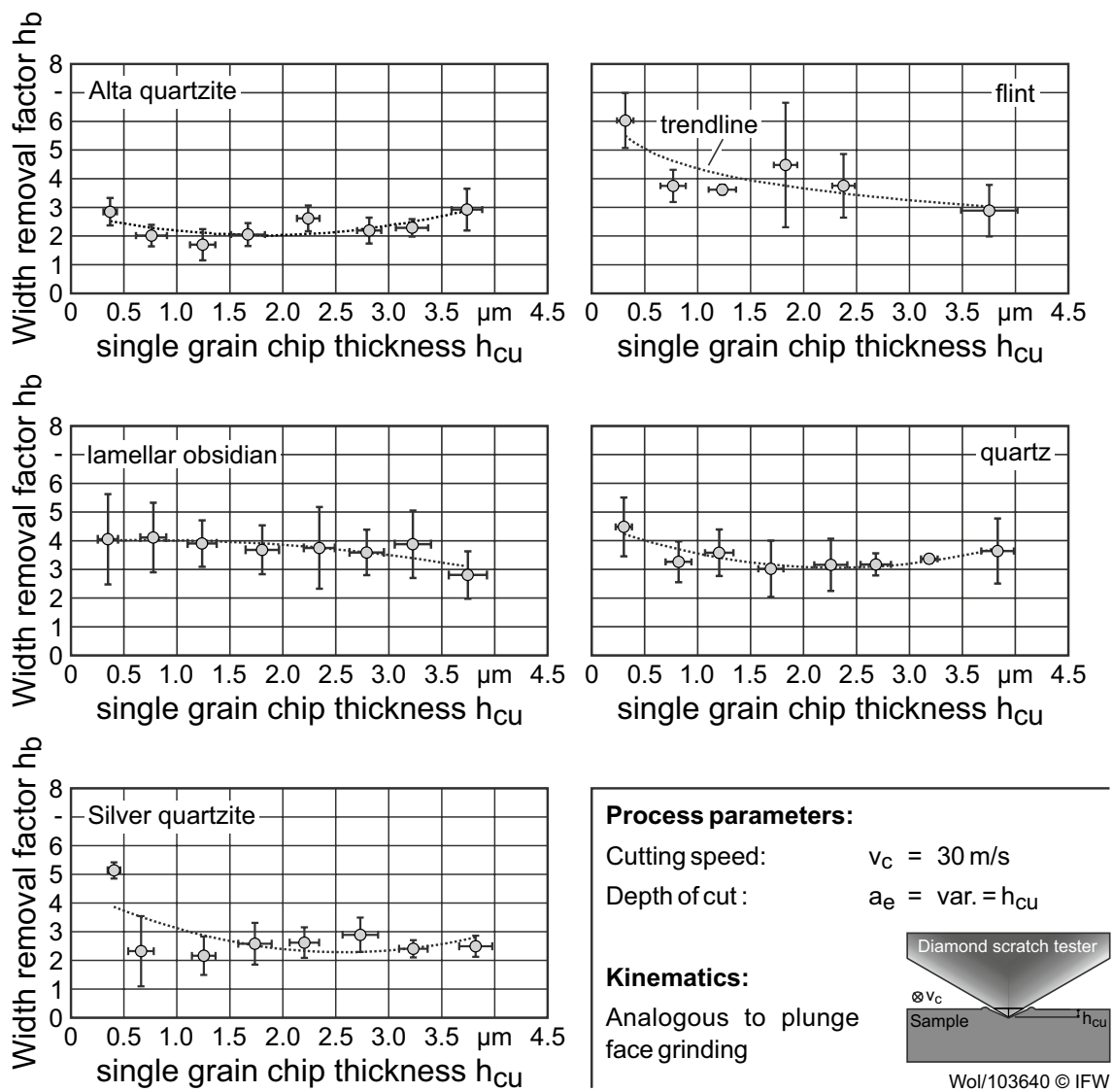


Fig. 6 Width removal factors of the rocks for different single grain chip thicknesses at a cutting speed of 30 m/s

of the single grain chip thickness influences these stress states, since a change in the penetration depth of the diamond tip into the material and a change in the amount of material to be removed changes the load at the diamond tip and in the material and thus also the stress state at these effective partners. Exceeding the range around the critical chip thickness would then lead to brittle material removal as a result of exceeding the load-bearing capacity of the material. Falling below critical chip thickness too far would also result in brittle material removal due to insufficient load and thus the absence of the stress state required for plasticisation of the rock. However, not only single grain chip thickness but also cutting speed influences the width removal factor and thus material removal as can be seen in Fig. 7 for Silver quartzite.

Two effects can be observed for a change of cutting speed for this rock: For the lower cutting speed of 15 m/s, higher values for  $h_b$  are received in the interval of the single grain chip thickness from 0 to 1.5  $\mu\text{m}$  compared to a cutting speed of 30 m/s. The width removal factor is up to 2.4 times higher for the lower cutting speed in this interval. This means that in correlation with cutting speed, a higher amount of brittle material removal can be expected for Silver quartzite under the given conditions. Afterward, the values of  $h_b$  are in a similar range for both cutting speeds indicating a comparable way of material removal. On the other hand, a steeper decrease of  $h_b$  can be observed for the lower cutting speed as well as a shift of the minimum of  $h_b$  to a higher single grain chip thickness (2.3  $\mu\text{m}$  for  $v_c = 15 \text{ m/s}$ , 1.3  $\mu\text{m}$  for  $v_c = 30 \text{ m/s}$ ). This indicates a more

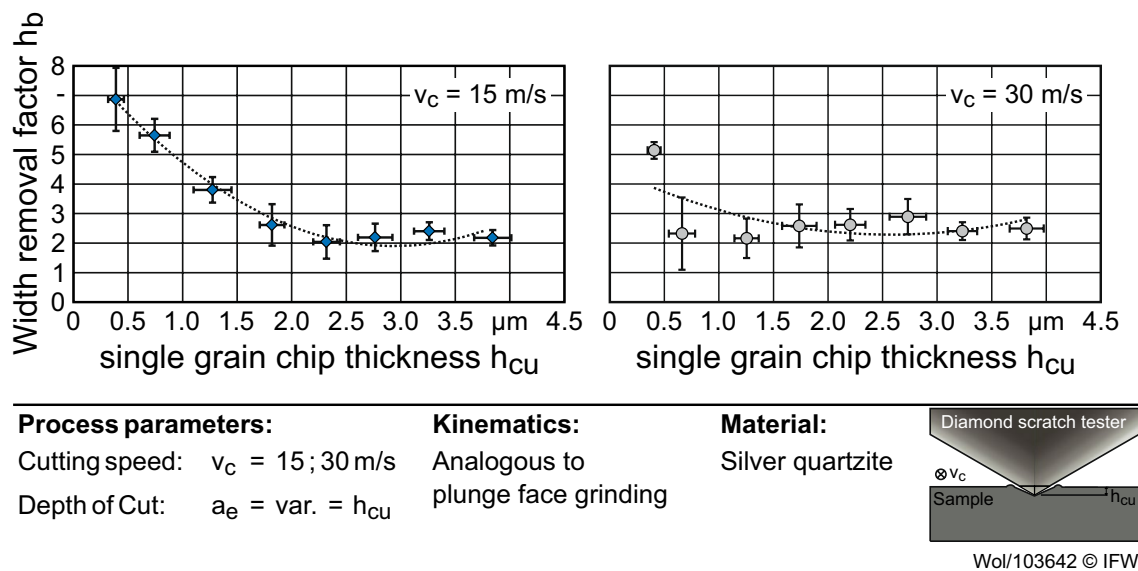


Fig. 7 Influence of cutting speed on width removal factor for Silver quartzite

pronounced change in material removal than for the higher cutting speed. Transferred to the design of tool grinding processes, this would mean that the grinding tool specifications and the remaining process parameters should be selected depending on the cutting speed in order to realise the highest possible proportion of ductile material removal and thus the lowest possible damage to the workpiece in the grinding process.

The observed effects can be explained by two factors. The first is the change in the momentum of the scratch tester correlating with the change in cutting speed. Because the mass of the scratch tester and the remaining moving parts of the experimental setup are not significantly changed, the momentum of the scratch tester increases with an increase in cutting speed. An increased momentum relates to higher forces and higher kinetic energy, which is applied to the rock in the scratch test. This changes the load imposed on the rock and thus the stress state, especially at the cutting edge of the scratch tester and in the surrounding microstructure. Considering the above-mentioned relationships, it can be assumed that this change in load and stress state due to the change in momentum of the scratch tester, together with the influence of the single grain chip thickness on these factors, leads to the observed effects. For the case illustrated in Fig. 7, this would mean that for a cutting speed of 15 m/s, the hydrostatic stress state in the material is initially not sufficient to plasticise the material and allow ductile material removal leading to brittle material removal and high width removal factors. With an increase in single grain chip thickness, the load on the material increases, and the stress state gets closer to the state needed for ductile

material removal. This leads to a decrease of brittle material removal and  $h_b$  until the acting stress state is sufficient to plasticise the material and allow domination of ductile material removal. After that, no significant decrease of  $h_b$  can be observed. For a cutting speed of 30 m/s, this stress state is reached at lower single grain chip thicknesses due to the higher momentum of the scratch tester. Therefore, ductile material removal starts at lower single grain chip thicknesses and quickly reaches  $h_b$  values comparable to those achieved with a cutting speed of 15 m/s.

A second possible factor is a change in the thermal load connected with the change in cutting speed. The thermal load in the contact zone between the scratch tester and the rock sample may increase for higher cutting speeds due to the higher relative velocity between them. Higher temperatures in the contact zone can promote ductile material removal and can influence the mechanical properties of the materials, as is shown above for the hardness and critical bending strength of the rocks. In addition, it is conceivable that the stress state in the contact zone is influenced by superimposing thermally induced stresses. But it must be mentioned that correlations between cutting speed and thermal loads can be complex and are not necessarily linear. The mentioned conceivable increase of thermal loads at higher cutting speeds must therefore be considered as a hypothesis until the acting thermal loads in the contact zone can be measured. However, the acting thermal loads in the contact zone were not covered in this investigation. Besides this, it must be mentioned that a possible influence of thermal loads on material removal could not be extensively pronounced because rocks are comparatively bad thermal conductors, and the contact

time between the rock sample and the scratch tester is very short. Therefore, the amount of thermal energy that can be transferred into the rock during contact with the scratch tester may be limited by these factors. This also limits the achievable rock temperature in the contact zone, and the influence of the thermal loads on material removal. However, without further investigations concerning the acting thermal loads in the contact zone the full extent of a possible thermal influence on material removal, in this case, remains unknown.

The effects described for Silver quartzite in connection with a change of cutting speed are not observable for all other investigated rocks. Figure 8 shows the influence of all cutting speeds on the width removal factor for all rocks investigated. For Alta quartzite, a comparable

influence of cutting speed on  $h_b$  as for Silver quartzite can be observed. As described before, the use of a cutting speed of 15 m/s leads to a shift of the minimum  $h_b$  to a higher single grain chip thickness for both quartzites. The trends for a cutting speed of 40 m/s are comparable to those described for both quartzites at a cutting speed of 30 m/s, although the decrease of  $h_b$  for an increase of single grain chip thickness is more pronounced in this case for Alta quartzite. As both rocks are quartzites, it can be assumed that the cause for this similarity in general behaviour is their similarity in diagenesis, while the observable differences in detail are caused by the different material properties. Different behaviour can be observed for flint. In this case, the lowest cutting speed of 15 m/s leads to a steeper decrease and lower  $h_b$ -values instead of the

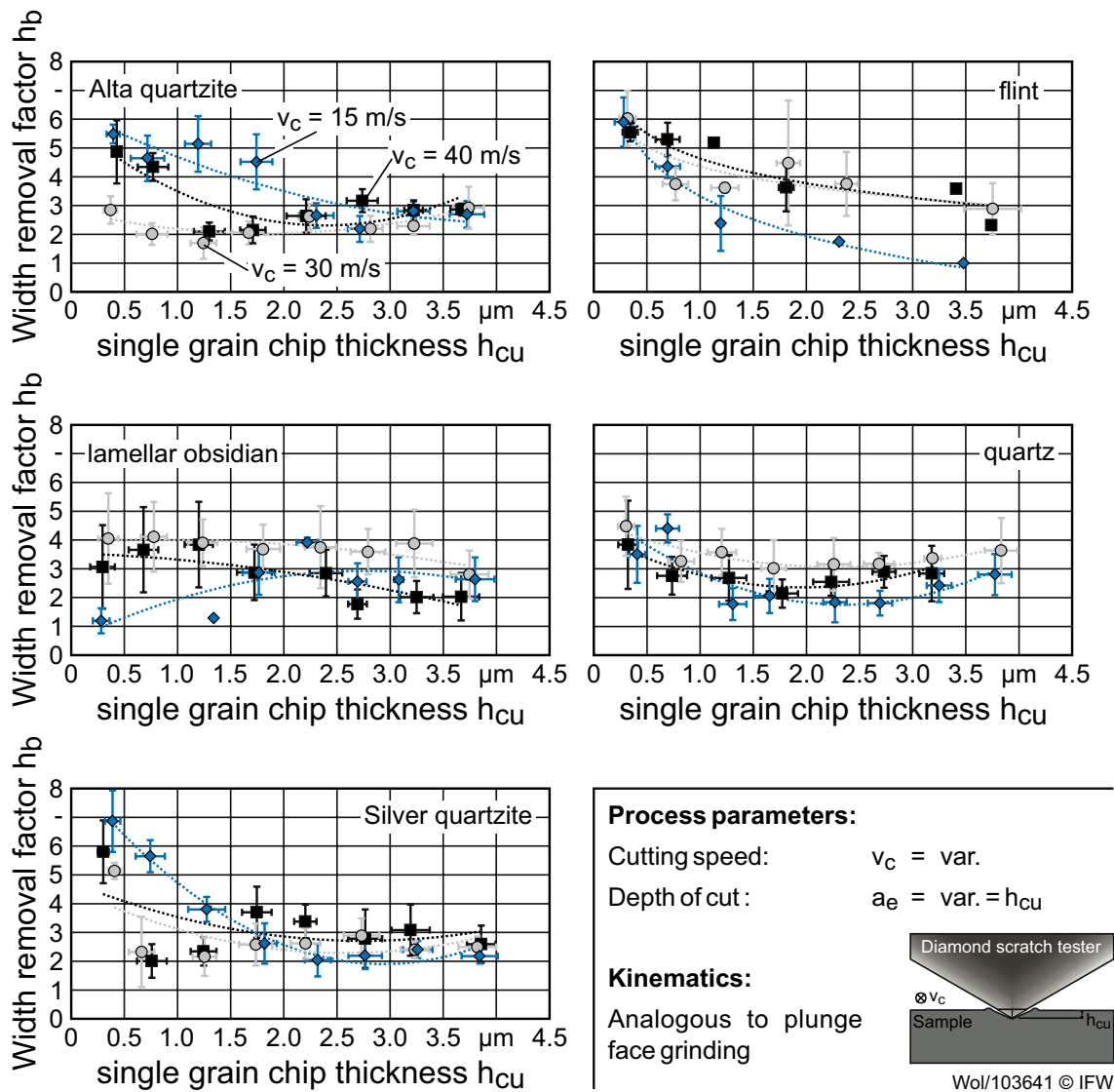
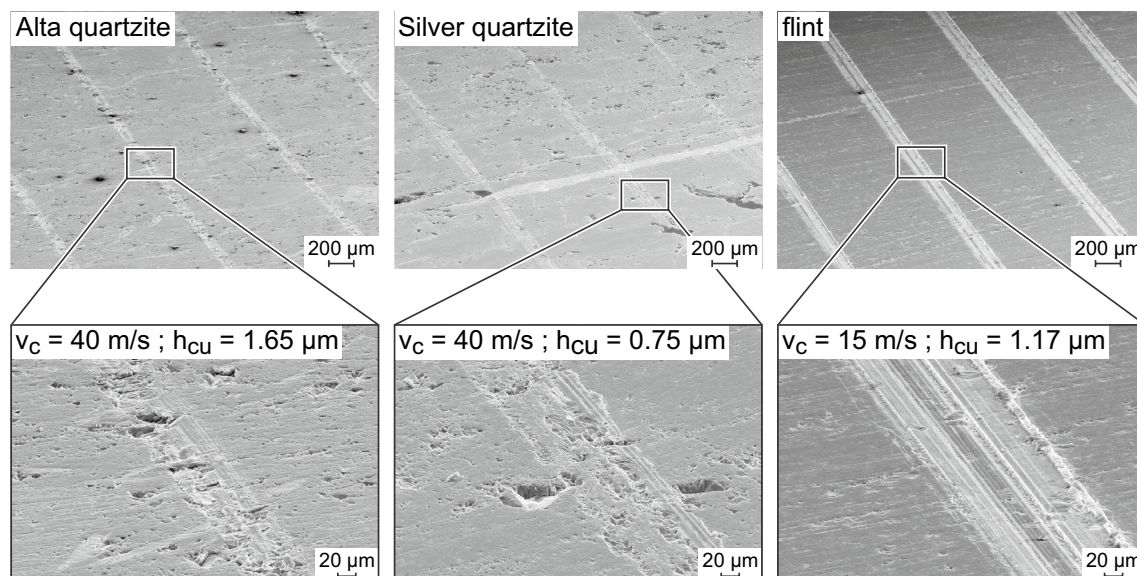


Fig. 8 Influence of cutting speed on width removal factor for all rock samples

higher cutting speeds for the quartzites. Besides that, no minimum of  $h_b$  followed by a renewed increase of  $h_b$  can be observed for all cutting speeds. As before, no signs for intensive brittle material removal could be detected for all cutting speeds for flint. The comparatively high  $h_b$ -values for lower single grain chip thicknesses could therefore be a result of ductile material displacements to the sides of the scratches, which would increase the width of the scratches and  $h_b$ . It is, therefore, possible that critical loads or stress states that would lead to brittle material removal are not reached under the given conditions. The high critical bending strength and fracture toughness of flint in comparison rocks that facilitate ductile material removal is a possible explanation for the observed differences to the other rocks. The finer grain size of flint in comparison to the quartzites already described in [6] can also contribute to this. Furthermore, it is possible that at the lowest cutting speed, a smaller amount of rock grains is displaced to the sides of the scratch tester than at higher cutting speeds, comparable to the formation of a bow wave of a ship at different speeds. For quartz, however, the results show no pronounced influence on the general behaviour of material removal. Instead, a change of cutting speed only reduces the  $h_b$ -values and shifts the minimum of  $h_b$ . The fact that a cutting speed of 30 m/s results in higher  $h_b$ -values for quartz than cutting speeds of 15 m/s or 40 m/s indicates the development of an unfavourable stress state in the material, which favours brittle material removal.

The amorphous lamellar obsidian shows a clearly different behaviour when the cutting speeds are varied, which

also differs from the other rocks. In this case, the use of a cutting speed of 15 m/s leads to an increase of  $h_b$ -values starting from values that indicate nearly optimal ductile material removal, while for the higher cutting speeds a decrease of  $h_b$  values can be observed, starting from values that indicate a much higher amount of brittle material removal. Amorphous materials such as glass have comparatively low critical single grain chip thicknesses. It is therefore assumed here that at a cutting speed of 15 m/s, the critical single grain chip thickness and the associated stress state in the material are quickly reached. This results in increasing amounts of brittle material removal and higher  $h_b$ -values for higher single grain chip thicknesses. The higher  $h_b$ -values for both higher cutting speeds at lower single grain chip thicknesses show that the amount of ductile material removal is much lower under these conditions and brittle material removal, therefore, more likely. But the decrease of  $h_b$  for the higher cutting speeds at higher single grain chip thicknesses indicates that an increase of the amount of ductile material removal is possible if a suitable stress state is induced onto the material. Therefore, the decrease of  $h_b$  is steeper for 40 m/s than for 30 m/s due to the higher momentum in this case and the correlating higher load and stress. As a general result, it can be stated that not only does single grain chip thickness influence the material removal of the rocks in the scratch tests but also the chosen cutting speed. The results indicate different influences of cutting speed on material removal depending on the used rock. Regarding the design of tool grinding processes of rock tools, this means that not only single grain chip thickness but also

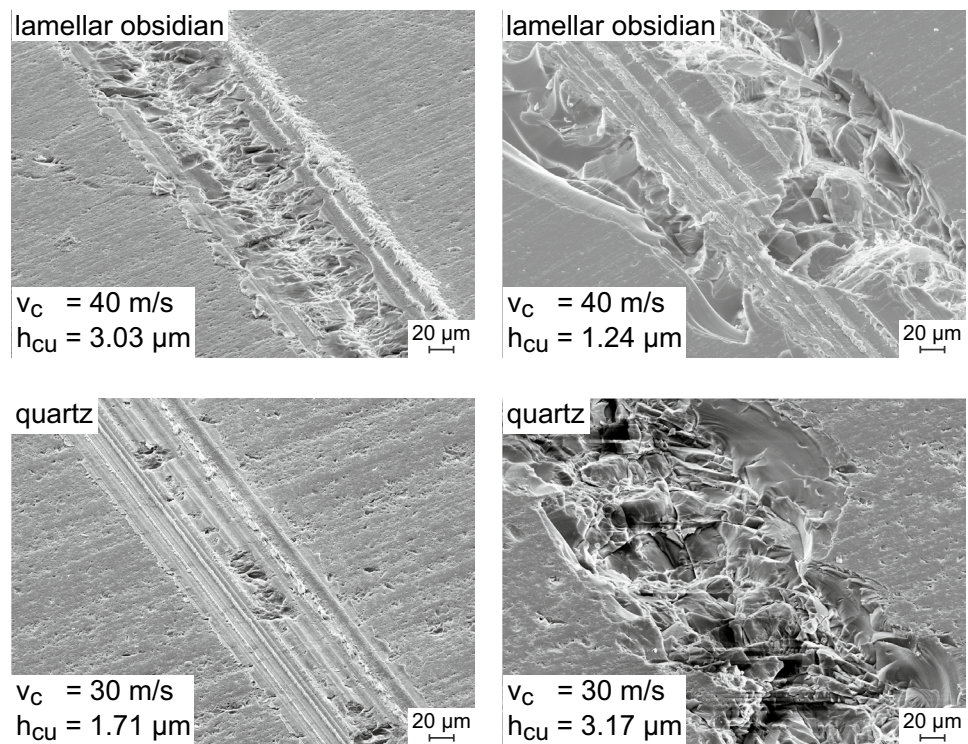


Wol/103590 © IFW

Fig. 9 SEM-images of scratches in flint and the quartzites



**Fig. 10** SEM-images of scratches in obsidian and quartz



Wol/103643 © IFW

cutting speed and the rock to be machined must be considered in the design of the tool grinding process.

As mentioned before, the described effects can also be found in SEM-images of the scratches, as can be seen in Figs. 9 and 10. Parameter combinations that show a low width removal factor also show comparatively smooth scratches with a low amount of brittle outbreaks at their sides, as can be seen in Fig. 9 for scratches in flint and the quartzites and Fig. 10 (left side) for lamellar obsidian and quartz. Regarding combinations that show higher width removal factors, the SEM-images also show the expected brittle material removal, as can be seen exemplarily in Fig. 10 (right side) for lamellar obsidian and quartz. The shell-shaped ruptures typical for these rocks at the sides of the scratch as though as further brittle outbreaks indicate the expected brittle material removal. Besides that, the material accumulations described before can be seen in Fig. 9 for flint on the right side of the scratch or in Fig. 10 in the image at the upper left for obsidian. However, although the general form of the scratches in Fig. 9 hints at a mainly ductile material removal, there are local signs for local brittle material removal. Examples of this are the brittle outbreaks within the scratches which can be found in the quartzites in Fig. 9 or Fig. 10 within the scratches of obsidian and quartz on the left. These phenomena may indicate a local deviation from the stress state in the

material needed for brittle material removal in front of the diamond tip. Likewise, these brittle outbreaks may be the result of elastic relaxation behind the diamond tip. But whether these brittle material removal phenomena in the scratches take place in front of or behind the diamond tip cannot be conclusively determined based on the present results. The fact that this brittle material removal inside the scratch does not necessarily influence the width of the scratch shows, however, that it must be considered that the width removal factor does not give precise information about the proportions of ductile or brittle material removal. Instead, it indicates which of these mechanisms dominates.

To allow a transfer of the results to the design of grinding processes of rock tools, the single grain chip thickness  $h_{cu,hbmin}$  that leads to a minimal width removal factor in the scratch tests is shown in Table 4 with the respective standard deviation. Since a minimum  $h_b$ -value favours ductile material removal, this parameter could be used for the design of tool grinding processes by using already existing single grain chip thickness models for the choice of process parameters. Furthermore, Table 4 gives the critical single grain chip thickness  $h_{cu,crit}$  according to Bifano [9], which describes the value at which a change in the material removal mechanisms occurs, to allow a comparison of the experimentally determined values of  $h_{cu,hbmin}$  with an established analytical model from the literature.

**Table 4** Values of the experimentally determined  $h_{cu,hbmin}$  and the analytically calculated  $h_{cu,crit}$

Rock	$h_{cu,hbmin}$ in $\mu m$			$h_{cu,crit}$ according to Bifano in $\mu m$
	$v_c = 15$ m/s	$v_c = 30$ m/s	$v_c = 40$ m/s	
Alta quartzite	$2.71 \pm 0.11$	$1.24 \pm 0.12$	$1.3 \pm 0.15$	0.05
flint	$3.48 \pm 0.03$	$3.75 \pm 0.27$	$3.74 \pm 0.02$	0.13
lamellar obsidian	$0.28 \pm 0.08$	$3.75 \pm 0.18$	$2.69 \pm 0.09$	0.09
quartz	$1.31 \pm 0.13$	$1.69 \pm 0.12$	$1.77 \pm 0.15$	0.02
Silver quartzite	$2.32 \pm 0.12$	$1.25 \pm 0.11$	$0.76 \pm 0.14$	0.03

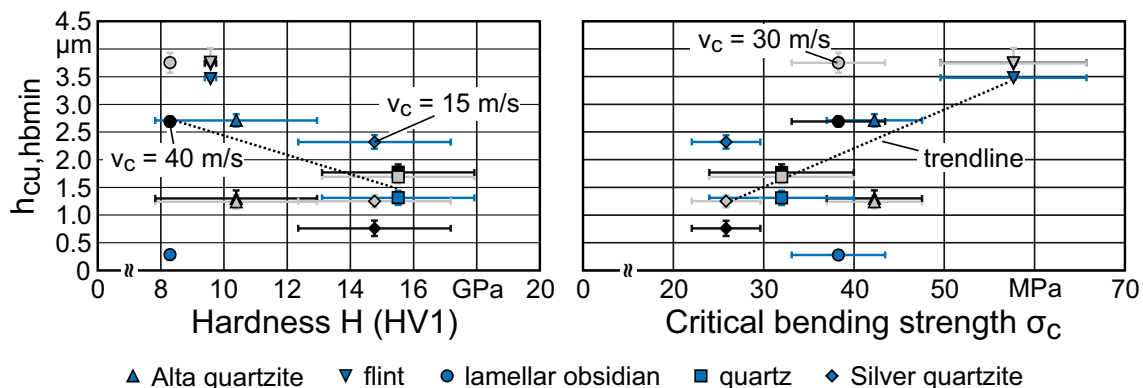
The critical single grain chip thickness can be calculated with Eq. (5) using Young’s modulus, the hardness, and the fracture toughness of the material [9]. The respective values of the rocks at 25 °C are used to calculate the values of  $h_{cu,crit}$  in Table 4.

$$h_{cu,crit} = 0.15 \cdot \left(\frac{E}{H}\right) \times \left(\frac{K_{Ic}}{H}\right)^2 \tag{5}$$

The comparison of the experimentally determined  $h_{cu,hbmin}$  and the analytically calculated  $h_{cu,crit}$  shows that  $h_{cu,hbmin}$  is between three and 87-times higher than  $h_{cu,crit}$ . Since ductile removal could be observed in all rocks despite the clear exceeding of  $h_{cu,crit}$ , this characteristic value established in the literature may not necessarily be a suitable parameter for the design of a tool grinding process of rock tools where ductile material removal mechanisms dominate. Furthermore, the analytical model does not consider the observed influence of cutting speed. It could therefore be advisable to develop new analytical models for the description of the critical single grain chip thickness in tool grinding of rocks or for the grinding of rocks in general based on future research projects. However, the trends that can be expected based on Eq. (5) for  $h_{cu,crit}$  can also be found

for  $h_{cu,hbmin}$ , as shown in Fig. 11. In Fig. 11,  $h_{cu,hbmin}$  is shown as a function of hardness and critical bending strength. It can be seen that there is a trend to a lower  $h_{cu,hbmin}$  for an increase in hardness and a trend to higher  $h_{cu,hbmin}$  for an increase in critical bending strength. The same tendency as for critical bending strength can be found between  $h_{cu,hbmin}$  and fracture toughness. For Young’s modulus, a tendency for  $h_{cu,hbmin}$  can also be observed, which is comparable to the mentioned tendency between hardness and  $h_{cu,hbmin}$ . Therefore, it can be assumed that although the analytically calculated critical chip thickness,  $h_{cu,crit}$  cannot be used for the design of tool grinding processes of rocks. The fundamental relationships underlying the considerations in this context are still valid in principle and can and should be taken into account in the process design. This means that rocks with high hardness and low toughness should be ground with a lower single grain chip thickness to maximise ductile material removal, while rocks with a high toughness should be ground with a higher single grain chip thickness.

However, it must be mentioned that there are differences between single grain engagements and multiple grain engagements that can influence the occurring material removal mechanisms. Although scratch tests make it possible to investigate the engagement of a single grain in



Wol/103603 © IFW

**Fig. 11** Influence of hardness and critical bending strength on  $h_{cu,hbmin}$

the material and the resulting material removal, it must be taken into account that in real grinding processes, a high number of grain engagements always occur simultaneously. Each grain acting in the grinding process induces a mechanical load into the material and influences its local stress state. It is therefore possible that a new stress state is created by superimposition which can facilitate ductile material removal in the case of small single grain chip thicknesses. The difference in grain protrusions present in real grinding tools is also an influencing factor that should not be neglected in such considerations. Different grain protrusions can lead to differences in their depth of cut and, therefore, to different single grain chip thicknesses and different local mechanical loads. Besides that, the contact conditions between the abrasive grains and the material can also be influenced by the grain shapes and their wear. Furthermore, it must be considered that multiple grain engagements can influence thermal loads in comparison to single grain engagement, such as by influencing the heat transfer between grinding tool and workpiece or through superposition of the influence of the heat sources that each grain engagement represents. Since the mentioned points cannot be properly investigated in scratch tests due to the engagement of a single grain in these cases, it should be mentioned that the results of this investigation may not be transferable in all points to real tool grinding processes. Quick-stop experiments like those presented in [17] could represent a way to investigate the influence of the factors described above and could further enhance the understanding of material removal mechanisms in tool grinding of rocks if the method is adapted to plunge face grinding processes. It can therefore be presumed that the implementation of such studies in future research projects could expand the state of the art in this respect and make important contributions to the development of analytical models to describe the processes.

Based on the results of this investigation, the following recommendations for the design of tool grinding processes of rock tools can be given. The process should be individually designed for each rock to be machined. The single grain chip thickness can be used as a guideline in the design process to maximise the amount of ductile material removal. For the rocks used in this investigation, a single grain chip thickness around the individual  $h_{cu,hbmin}$  should be chosen for this purpose. It must be taken into account that not only the single grain chip thickness influences the material removal behaviour of the rocks but also the cutting speed. This also applies to  $h_{cu,hbmin}$ . Therefore, both factors should be considered in the design of the grinding process and adjusted individually to the rocks. Furthermore, it should be considered that the area of single grain chip thicknesses suitable for ductile material removal can be underestimated by established analytical

models. The use of single grain chip thicknesses calculated with these models in the process design could then favour brittle material removal as a result of an unsuitable stress state in the rock induced by a low single grain chip thickness. In general, it can be recommended to increase single grain chip thickness for the machining of tougher rocks and to decrease it for harder rocks with a lower toughness to favour ductile material removal.

But for the design of a grinding process, the following points should also be considered based on the presented results. Ductile material removal in tool grinding of hard and brittle cutting tool materials is not the only factor of significance. It is also important to manufacture a tool with a cutting edge of high quality and low cutting-edge roughness. High single grain chip thicknesses have the potential to increase the cutting-edge roughness and, therefore, to reduce the quality of the cutting-edge or even to damage it. Furthermore, it must be mentioned that the single grain chip thicknesses found to be beneficial for ductile material removal in the scratch test are unusually high for tool grinding processes due to the usually applied parameter combinations and grinding tool specifications in these processes. The use of grinding tools with higher grain sizes and lower grain concentrations would pose a possibility to reach the required single grain chip thicknesses, but at the same time, this could lead to an increase in cutting-edge roughness. Therefore, investigations of the cutting-edge quality are needed to evaluate whether a sufficient cutting-edge quality is achieved or whether further subsequent process steps like the application of a cutting-edge rounding are necessary and possible. In addition, it must be considered that the scratch tests cannot take into account the effect of a simultaneous engagement of multiple abrasive grains in the material, which is typical for grinding processes. As a simultaneous grain engagement can influence the stress state in the material due to the additional local load sources, it cannot be ruled out that the single grain chip thickness for an optimal amount of ductile material removal could differ from the values evaluated in this investigation. Quick-stop experiments such as those presented in [17] would be required to evaluate the influence of multiple grain engagements on material removal in these cases.

For the design of a tool grinding process of the rocks examined in this paper, the results would mean that Alta-quartzite should be ground with a cutting speed of 30 m/s and a single grain chip thickness of around 1.24  $\mu\text{m}$  to maximise the amount of ductile material removal. For Silver quartzite, the same applies to a cutting speed of 40 m/s and a single grain chip thickness of 0.76  $\mu\text{m}$ . For lamellar obsidian and quartz, a lower cutting speed of 15 m/s should be chosen to achieve this. A single grain chip thickness around 1.31  $\mu\text{m}$  similar to the quartzites

should be chosen for the machining of quartz, while a much lower single grain thickness around 0.28  $\mu\text{m}$  would be suitable for machining lamellar obsidian at this cutting speed. Since the results show mainly ductile material removal for flint independent from the chosen parameter combination and despite high  $h_b$ -values, it can only be recommended to choose a cutting speed of 15 m/s to decrease the amount of material, which is displaced to the side of the cutting edge and to favour chip formation in front of the cutting edge.

## 4 Conclusions

In this paper, the influence of cutting speed and single grain chip thickness on material removal of five rocks are investigated via scratch tests in analogy to a face plunge grinding process. The aim of this paper is to improve the understanding of tool grinding processes of rock tools to contribute to a knowledge-based design of these processes. For this reason, the rock properties are investigated by hardness measurements, nanoindentation, Palmqvist tests, and three-point bending tests. Scratch-tests analogous to the kinematic and contact conditions of a face plunge grinding process are performed under variation of cutting speed and single grain chip thickness. The occurring material removal mechanisms are analysed using SEM-images and a confocal microscope. Based on the results of this investigation, the following conclusions can be drawn:

- It is possible to achieve dominance of ductile material removal for all rocks in the scratch tests.
- Cutting speed and single grain chip thickness influence the occurring and dominating material removal mechanism. However, the results show an interaction between these two parameters concerning the occurring material removal mechanism.
- The width removal factor  $h_b$  can be used to identify parameter setups that favour ductile material removal. The respective setups to achieve this differ for the individual rocks.
- The evaluated single grain chip thicknesses for ductile material removal are up to 87-times higher than predicted by an established analytical model. The single grain chip thicknesses found to favour ductile removal mechanisms are very high for conventional tool grinding processes.
- The results allow the first steps towards a knowledge-based design of grinding processes of rock tools. Nevertheless, further investigations on the influence of the simultaneous engagement of multiple abrasive

grains occurring during grinding and on the influence of the selected process parameters and the grinding tool specifications on the cutting edge quality have the potential to expand this knowledge base. The conduction of such investigations is therefore recommended in order to be able to ensure the transferability of the knowledge gained to the tool grinding process as well as to industrial applications.

**Acknowledgements** The authors would like to thank the German Research Foundation (DFG) for supporting the project BR 2967/12-1 “Manufacturing and operational behaviour of cutting tools made of rock”.

**Authors' contribution** BB was responsible for funding acquisition and project supervision. He also reviewed and edited the manuscript in the writing process together with BD and BB, PW conducted the experiments, analysed the data and wrote the manuscript. He was also responsible for project administration together with BB.

**Funding** Open Access funding enabled and organized by Projekt DEAL. This work was supported by the German Research Foundation (DFG) under grant number BR 2967/12-1.

## Declarations

**Conflict of interest** This work was supported by the German Research Foundation (DFG) under grant number BR 2967/12-1. The funders had no role in the design of this work, in the collection, analyses, and interpretation of the data, in the writing of the manuscript, or in the decision to publish the results. On behalf of all authors, the corresponding author states that the authors have no competing interests to declare that are relevant to the content of this article.

**Open Access** This article is licensed under a Creative Commons Attribution 4.0 International License, which permits use, sharing, adaptation, distribution and reproduction in any medium or format, as long as you give appropriate credit to the original author(s) and the source, provide a link to the Creative Commons licence, and indicate if changes were made. The images or other third party material in this article are included in the article's Creative Commons licence, unless indicated otherwise in a credit line to the material. If material is not included in the article's Creative Commons licence and your intended use is not permitted by statutory regulation or exceeds the permitted use, you will need to obtain permission directly from the copyright holder. To view a copy of this licence, visit <http://creativecommons.org/licenses/by/4.0/>

## References

1. Furberg A, Arvidsson R, Molander S (2019) Environmental life cycle assessment of cemented carbide (WC-Co) production. *J Clean Prod* 209:1126–1138
2. European Commission (2017) Communication from the commission to the European parliament, the council, the European economic and social committee and the committee of the regions on the 2017 list of critical raw materials for the EU. Brussels
3. European Commission (2018) Report on critical raw materials in the circular economy. Brussels



4. Al Barazi S (2018) Rohstoffrisikobewertung—Kobalt—DERA Rohstoffinformationen, vol 36. Berlin
5. Werner ABT, Sinclair WD, Amey EB (2014) International strategic mineral issues summary report—Tungsten (Ver. 1.1, November 2014). U.S. Geological Survey Circular 930-O. U.S. Department of the Interior, Reston, VA
6. Denkena B, Breidenstein B, Krödel A, Picker T, Wolters P (2022) Suitability of natural rocks as materials for cutting tools. *SN Appl Sci* 4:2. <https://doi.org/10.1007/s42452-021-04883-z>
7. Wolters P, Picker T, Breidenstein B, Krödel A, Denkena B (2022) Application of natural rocks in cutting aluminum. In: Behrens BA, Brosius A, Drossel WG, Hintze W, Ihlenfeldt S, Nyhuis P (eds) *Production at the leading edge of technology*. WGP 2021. Lecture notes in production engineering. Springer, Cham. [https://doi.org/10.1007/978-3-030-78424-9\\_26](https://doi.org/10.1007/978-3-030-78424-9_26)
8. Inasaki I (1987) Grinding of hard and brittle materials. *CIRP Ann Manuf Technol* 36(2):463–471
9. Biffano TG (1988) Ductile-regime grinding of brittle materials. North Carolina, North Carolina State University, PhD-Thesis
10. Malkin S, Ritter JE (1989) Grinding mechanisms and strength degradation for ceramics. *J Eng Ind* 111(2):167–174
11. Hessert R (1998) Bearbeitungsspannungen, Randschichtschädigungen und Festigkeiten geschliffener  $Al_2O_3$ - und  $ZrO_2$ -Keramiken. Dr.-Ing. Dissertation, Karlsruhe, Universität Karlsruhe (TH)
12. Lawn BR, Wilshaw TR (1975) Indentation fracture: principles and applications. *J Mater Sci* 10(6):1049–1081
13. Lawn BR, Swain MV (1975) Microfracture beneath point indentation in brittle solids. *J Mater Sci* 10(1):113–121
14. Malkin S, Hwang TW (1996) Grinding mechanisms for ceramics. *CIRP Ann* 45(2):569–580
15. Busch DM (1968) Ritz- und Verschleißuntersuchungen an spröden Werkstoffen mit einzelkornbestückten Hartstoffwerkzeugen, Dr.-Ing. Dissertation, Hannover, Technische Hochschule Hannover
16. Zhang Z, Wang B, Kang R, Zhang B, Guo D (2015) Changes in surface layer of silicon wafers from diamond scratching. *CIRP Ann Manuf Technol* 64:349–352
17. Denkena B, Krödel A, Wippermann A, Wolters P (2020) Grinding of transformation-toughened mixed oxide ceramic. *Int J Adv Manuf Technol* 109:1463–1478
18. Nishimatsu Y (1972) The mechanics of rock cutting. *Int J of Rock Mech Min Sci* 9(2):261–270
19. Richard T, Dagrain F, Poyol E, Detournay E (2012) Rock strength determination from scratch tests. *Eng Geol* 147–148:91–100
20. Garner NE (1967) Cutting action of a single diamond under simulated borehole conditions. *J Petrol Technol* 19:937–942
21. Wang CY, Clausen R (2002) Marble cutting with single point cutting tool and diamond segments. *Int J Mach Tools Manuf* 42(9):1045–1054
22. Miedema SA (2014) *The delft sand*. IOS Press, Amsterdam, Clay & Rock Cutting Model
23. Meding M (1993) Beschreibung des Prozeßgeschehens bei der Zerspanung von Gestein und von dessen bruchmechanischem Verhalten unter besonderer Berücksichtigung der Schallemissionsanalyse. Dr.-Ing. Dissertation, Hamburg, Technische Universität Hamburg-Harburg
24. Huang H, Lecampion B, Detournay E (2013) Discrete element modelling of tool-rock interaction I: rock cutting. *Inter J Numer Anal Meth Geomech* 37:1913–1929
25. Mohammadnejad M, Dehkhoda S, Fukuda D, Liu H, Chan A (2020) GPGPU-parallelised hybrid finite-discrete element modelling of rock chipping and fragmentation process in mechanical cutting. *J Rock Mech Geotech Eng* 12:310–325
26. Kalyan B, Murthy ChSN, Choudhary RP (2015) Rock indentation indices as criteria in rock excavation technology—a critical review. *Proc Earth Planet Sci* 11:149–158
27. Altindag R, Güney A (2006) ISRM suggested method for determining the shore hardness value for rock. *Int J Rock Mech Min Sci* 43:19–22
28. Meng F, Wong LNY, Zhou H (2021) Rock brittleness indices and their applications to different fields of rock engineering: a review. *J Rock Mech Geotech Eng* 13:221–247
29. Ulusay R, Hudson JA (eds) (2007) *The complete ISRM suggested methods for rock characterization, testing and monitoring: 1974–2006*. International Society for Rock Mechanics
30. Deutsches Institut für Normung (2008) *Advanced technical ceramics—mechanical properties of monolithic ceramics at room temperature—part 1: determination of flexural strength*. German version EN 843-1:2006. DIN Deutsches Institut für Normung e.V., Berlin
31. Denkena B, Grove T, Bremer I, Behrens L (2016) Design of bronze-bonded grinding wheel properties. *CIRP Annals – Manufacturing Technology* 65: pp. 333–336
32. Deutsches Institut für Normung (2016) *DIN ISO 21940–11: Mechanical vibration—Rotor balancing—part 11*. Deutsches Institut für Normung e.V., Berlin
33. Apmann H (2004) *Seilschleifen von metallischen und mineralischen Werkstoffen*, Dr.-Ing. Dissertation, Hannover, Universität Hannover
34. Carter CB, Norton MG (2007) *Ceramic materials—science and engineering*. Springer Science + Business Media, New York, NY
35. Salmang H, Scholze H, Telle R (2007) *Keramik*. Springer-Verlag, Berlin

**Publisher's Note** Springer Nature remains neutral with regard to jurisdictional claims in published maps and institutional affiliations.